Reconnection Signatures in Kelvin Helmholtz Instability in PIC Simulations

Narges Ahmadi[1], Frederick D. Wilder[2], Robert E. Ergun[1], David Newman[1], Yi Qi[1], Kai Germaschewski[3], Stefan Eriksson[1], Alexandros Chasapis[1]and Scot Elkington[1]

[1]Laboratory of Atmospheric and Space Physics, University of Colorado Boulder, Boulder, Colorado, USA
[2]University of Texas at Arlington, Department of Physics, Arlington, Texas, USA
[3]University of New Hampshire, Department of Physics, Durham, NH, USA

Key Points:

- Reconnection signatures are identified in Kelvin Helmholtz Instability using Magnetic Flux Transport, magnetic field topology and minimums.
- The reconnection signatures are at the edges of and within the vortex structures.
- The number of X-lines peak at the turbulence phase and decrease as instability becomes fully evolved and very turbulent.

Corresponding author: Narges Ahmadi, Narges.Ahmadi@colorado.edu

Abstract

We performed 2D PIC simulations of Kelvin Helmholtz instability (KHI) with symmetric and asymmetric density and temperature profiles along the flow shear with a northward interplanetary magnetic field. The Magnetic Flux Transport method, field topology and magnetic field minimums are used to identify the reconnection X-lines. We start to observe the reconnection signatures such as magnetic field and flow reversals at the vortex edges in the nonlinear phase of the KHI when the vortices are rolling up. The number of reconnection regions increases at the turbulence phase. The signatures eventually decrease and finally disappear at very turbulent stages of KHI developments. Our results qualitatively agree with MMS observations of reconnection signatures at KHI along the magnetospheric flanks.

Plain Language Summary

Kelvin Helmholtz instability forms at the boundary of flows moving in opposite directions. The instability forms ocean-like waves and vortices that roll up and become turbulent. This instability happens at the magnetopause boundary around the Earth where the shocked solar wind plasma meets magnetopsheric plasma with a flow shear. As the vortices roll up, they twist the magnetic field lines and can cause magnetic reconnection. Magnetic reconnection changes field topology and releases mass and momentum to the magnetosphere. We investigate the occurrence of reconnection in the Kelvin Helmholtz instability development using fully kinetic simulations. Our simulation results show that as Kelvin Helmholtz instability develops and becomes nonlinear, reconnection signatures start to appear. The reconnection signatures peak when instability is getting turbulent and they fade away at the very turbulent phases of the instability.

1 Introduction

The Kelvin-Helmholtz instability (KHI) which occurs in Earth's magnetospheric flanks is an important driver of mass and momentum transfer from the solar wind to the Earth's magnetosphere (Axford & Hines, 1961; Nykyri & Otto, 2001; Hasegawa et al., 2004; Kavosi & Raeder, 2015; Ma et al., 2017). Recent studies have proposed that magnetic reconnection in the KHI might facilitate this mass and momentum transfer (Nykyri & Otto, 2001; Nykyri et al., 2006; Hasegawa et al., 2009; Nakamura et al., 2013; Eriksson et al., 2016; Ma et al., 2017; Eriksson et al., 2021). The KHI is generated due to flow shear at the magnetopause boundary between the shocked solar wind or magnetosheath and magnetospheric plasma (Hasegawa et al., 2006; Johnson et al., 2014). The KHI results in surface waves that propagate anti-sunward down the magnetospheric flanks, and as the instability becomes nonlinear, the waves roll up and form vortices. These rolled up vortices can lead to compressed current sheets in converging flow regions at the spine regions or at the edge of the vortices. This is where magnetic reconnection can occur where opposing magnetic field lines meet (Nykyri & Otto, 2001; Nakamura et al., 2013). Simulations and MMS observations have also displayed that the vortices become turbulent as they roll up (Karimabadi et al., 2013; Nakamura & Daughton, 2014; Stawarz et al., 2016). This turbulence can transfer energy from the large-scale vortices to smaller scales where dissipative collisionless processes can heat the particles.

MMS observations by several studies (Eriksson et al., 2016; Stawarz et al., 2016) show signatures of current sheets that can support reconnection of the type predicted by Nakamura et al. (2013) called type-I reconnection. Nakamura et al. (2013) start the simulation with a reversing in-plane magnetic field of Harris type current sheet along the flow shear. Therefore, the in-plane magnetic field lines are naturally anti-parallel in spine regions of KHI and compressed field lines and currents sheets can lead to reconnection in those regions. Eriksson et al. (2016) reported that, for the 40 current sheets in the KHI

encountered by MMS on 8 September 2015, 20 showed evidence for reconnection ion jets. In addition to compressed current sheets flanking the vortices at spine regions, reconnection could also occur on thin current sheets within the turbulent region and inside the vortex roll up (Nykyri & Otto, 2001). In this case, the in-plane magnetic field is parallel across the magnetopuse boundary and a vortex roll up makes the magnetic field lines anti-parallel inside the vortex edges and consequently reconnection can occur. This is called type-II reconnection.

Wilder et al. (2023) investigated KHI events at different positions along the flank magnetopause (further down tail) using MMS data to determine if reconnection is also observed at other stages in the KHI's development, as well as the frequency of occurrence as they become increasingly rolled up and turbulent. They showed the fraction of current sheets, that exhibit reconnection signatures of type-I, decreases for events further down the magnetospheric flanks and it suggests that as the instability evolves into a very turbulent phase, reconnection becomes less prevalent.

In this paper, we investigate magnetic reconnection signatures at different stages of the KHI using data from local particle-in-cell (PIC) simulations and compare our results with those reported from MMS observations by (Wilder et al., 2023). The KHI is thought to drive magnetospheric convection (Axford & Hines, 1961; Kavosi & Raeder, 2015) in addition to reconnection at the dayside magnetopause and magnetotail, and therefore understanding of mass and momentum transfer via the instability is needed to predict its impacts on the system. These impacts are especially important during northward IMF conditions when reconnection at the sub-solar magnetopause is less likely.

2 Simulation Setup

In order to study magnetic reconnection signatures as KHI grows, we need a fully kinetic PIC code. The Plasma Simulation Code (PSC) is a state of the art PIC simulation code with advanced features like load-balancing and GPU support (Germaschewski et al., 2016). We initialize a system consisting of protons and electrons for a 2D configuration that is unstable to KHI following a modified setup described by Karimabadi et al. (2013). Using PSC, we will simulate the evolution of the KHI and track the development of X-lines and magnetic flux transports, which can be compared with the reported MMS observations.

We study two cases in this paper. First case is a symmetric density and symmetric temperature profile in the simulation box. The second case is an asymmetric density and asymmetric temperature profile across the flow shear resembling the changes in plasma parameters in the magnetopause boundary. These two cases give us the opportunity to compare the impact of the asymmetry on the reconnection signatures in the KHI. The simulations are 2 dimensional and in Y-Z plane. Initial condition for the symmetric density and symmetric temperature case is the following: The ion and electron temperatures are equal $T_i/T_e = 1$ and uniform in the simulation box, the $\omega_{pe}/\Omega_{ce} = 2$, $m_i/m_e = 100$, $n_{cell} = 150$ (number of particles per cell), $\beta = 0.1$ (total beta), simulation domain is $25d_i \times 50d_i$ $(Y \times Z)$ with the resolution of 4096×8192, periodic boundary conditions in $y = 0$ and $y = 25$ and reflecting boundary conditions for particles and conducting wall boundary conditions for electromagnetic fields at $z = 0$ and $z = 50$. ω_{pe} is electron plasma frequency and Ω_{ce} is electron cyclotron frequency. $d_i = c/\omega_{pi}$ is the ion inertial length with c being speed of light and ω_{pi} the ion plasma frequency.

The initial magnetic field is $B = B_0 \sin(\theta)\hat{x} + B_0 \cos(\theta)\hat{z}$. The ratio of magnetic fields is $B_x/B_z = 20$ with $\theta = 87°$. B is mostly out of the plane in the X direction with a small component in Z direction (X-Z Plane). The out of plane magnetic field in X direction plays the role of guide magnetic field for the in-plane magnetic reconnections during KHI evolution. This is equivalent of an equatorial plane with Earth's magnetic field

being out of the simulation plane and a northward interplanetary magnetic field. The flow shear is given by $v_z = v_{0z}\tanh[(y-0.5L_y)/\delta] + \delta_{vp}v_{0z}\sin(k_{vp}z/L_z)exp[-(y-0.5L_y)^2/\delta^2]$ where $L_y = 25d_i$, $L_z = 50d_i$, $\delta = 2$, $\delta_{vp} = 0.15$ and $k_{vp} = 0.5$. The shear in the flow is in Y direction. The initial electric field is $E = -v \times B = -v_z B_0 \sin(\theta)\hat{y}$ to sustain the equilibrium shear flow. Electrons are initialized slightly nonuniform to satisfy Gauss's law, since the convective electric field breaks the charge neutrality (Pritchett & Coroniti, 1984).

For the case of asymmetric density and asymmetric temperature, the resolution is 4000×8000 grid cells. The majority of the initial conditions are the same as previous case unless otherwise noted. The density profile is $n = n_{10}/2(1-\tanh[(y-0.5L_y)/\delta]) + n_{20}/2(1+\tanh[(y-0.5L_y)/\delta])$. Subscript 1 is the region on the left of simulation box (negative v_z flow) and subscript 2 is on the right side of the box where v_z flow is positive. To satisfy the total pressure balance (kinetic plus magnetic field), the temperature profile is $T_{i2}/T_{e2} = n_{i1}/n_{i2}[T_{i1}/T_{e2} + T_{e1}/T_{e2}] - 1$. We initially set $n_{10}/n_{20} = 2$ and $T_{e1}/T_{e2} = 0.5$. The left to right direction in the simulation box (in Y direction) represents a magnetosheath to magnetosphere crossing from higher density to lower density plasma and lower temperature to higher temperature. The magnetic field is out of the plane in the box, resembling a northward interplanetary magnetic field and Earth's magnetic field similar to the previous case. Figure 1 shows the initial conditions for both cases. The plots are velocity profile in Z direction, ion density, ion temperature and convective electric field in Y direction. The ion density and temperature in the bottom panel show the asymmetric case setup, resembling a magnetopause crossing.

3 Reconnection Signatures

We are interested in how the reconnection signatures in the KHI evolve at different stages of the instability's development. We use the Magnetic Flux Transport (MFT) method, magnetic field topology and finding minimums of in-plane magnetic field to identify the reconnecting current sheets and active reconnection sites. The MFT method was recently used in kinetic simulations of reconnection (Liu & Hesse, 2016; Liu et al., 2018). MFT considers the decoupling of the magnetic flux and the electron flow due to breaking of the frozen-in condition and presence of nonideal electric field. Therefore, MFT shows the inward and outward flow of magnetic flux at the reconnection X-point. $U_\Psi = cE_x/B_p(\hat{x} \times \hat{b_p})$ is the magnetic flux term where $\hat{x}$ is guide field direction, $\hat{b_p}$ is the unit vector of the in-plane magnetic field, B_p is the magnitude of the in-plane magnetic field and E_x is out of plane electric field. The MFT terms show the difference between magnetic flux and electron flow when electrons are not frozen-in to the magnetic field. This method has been used both in MMS observations and simulations of plasma turbulence (Li et al., 2021; Qi et al., 2022).

Figure 2 shows the MFT terms and its vector plot in the symmetric (top panel) and asymmetric (bottom panel) simulation cases. The $U_y = -cE_xB_z/B_p^2$ ($U_z = cE_xB_y/B_p^2$) plot shows the magnetic flux in Y (Z) direction. The red color indicates magnetic flux moving in +Y (+Z) and blue color is when the flux is moving in -Y (-Z) direction. The regions with sharp change in color (blue to red or red to blue) is where the flow reversal is happening. The inflow or outflow can be either in Y or Z direction or a combination of both. Depending on the directions of the reversals relative to each other, we can have an X-line. The X-lines are where we see converging inflows and diverging outflows. These X-lines regions are clearly seen in third column of figure 2 for both cases where we plot the in-plane magnetic field lines. The magnitude of the in-plane magnetic field is below 10^{-4} in these X-line regions (250 times smaller than the average in-plane magnetic field magnitude). The red stars show where the magnetic field lines are reconnecting. We observe 4 X-lines in the symmetric case at $\Omega_p t = 275$ and 5 X-lines in the asymmetric case at $\Omega_p t = 195$.

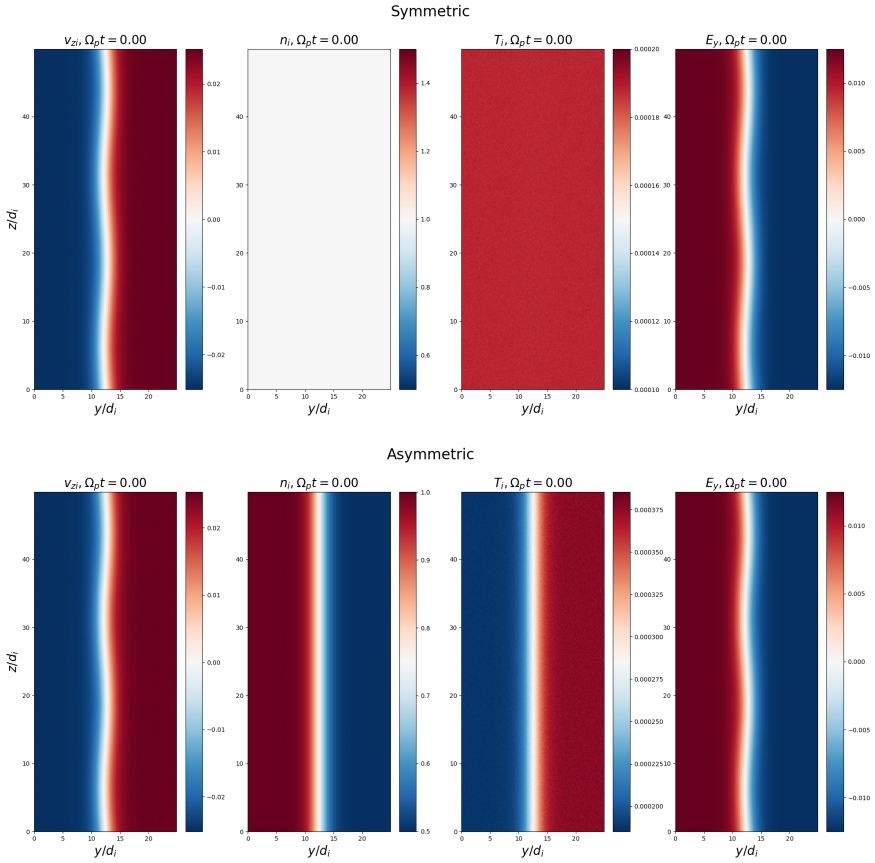

Figure 1: Initial conditions for two simulations cases: (top) Symmetric case (bottom) Asymmetric case. The plots are velocity profile in Z direction, ion density, ion temperature and convective electric field in Y direction. The ion density and temperature in the bottom panel show the asymmetric case setup, resembling a magnetopause crossing from magnetosheath to the inner magnetosphere.

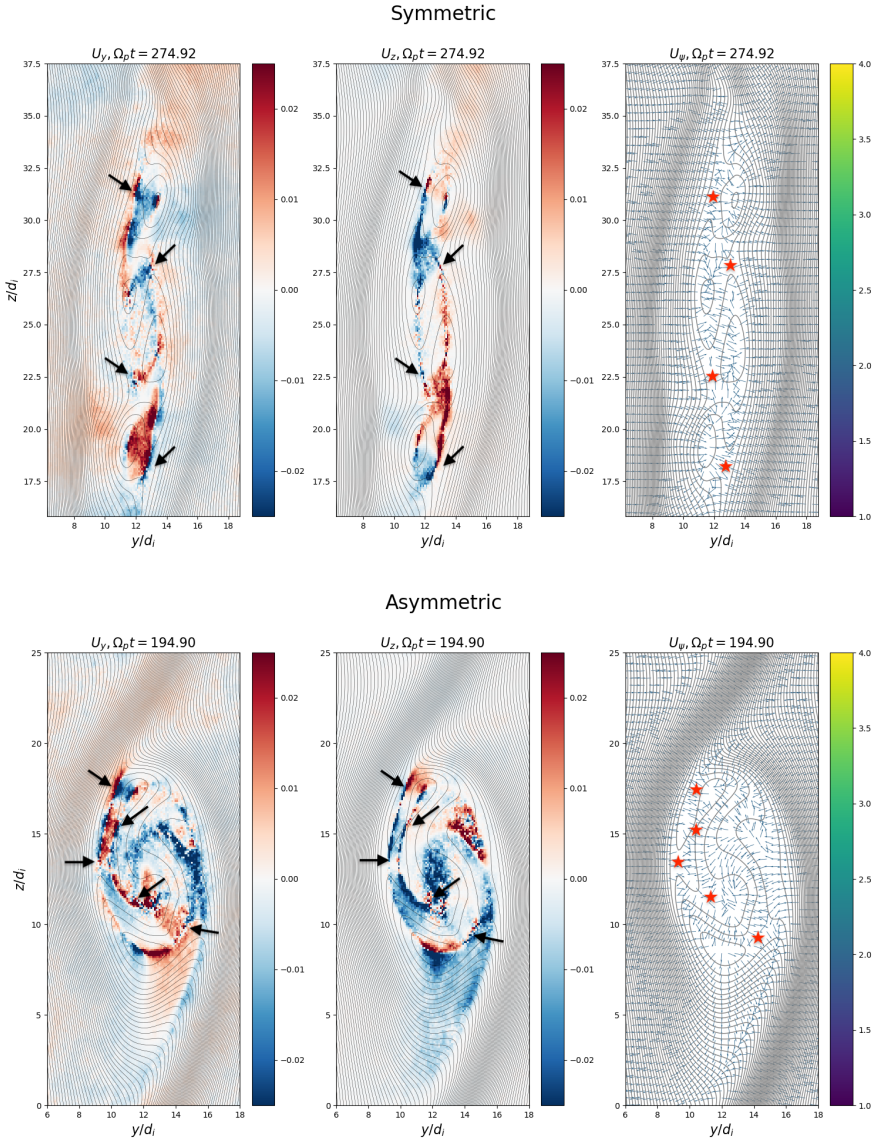

Figure 2: MFT terms and MFT vector for two simulations cases: (top) Symmetric case at $t = 275/\Omega_p$ (bottom) Asymmetric case at $t = 195/\Omega_p$. MFT shows the inflow and outflow flux transport regions near the X-lines. The black arrows point to flow reversals near the X-lines and red stars show the X-lines visible based on the in-plane magnetic field topology and magnetic field minimums. The arrows in the third column for both cases are the MFT vectors showing the direction of the magnetic flux.

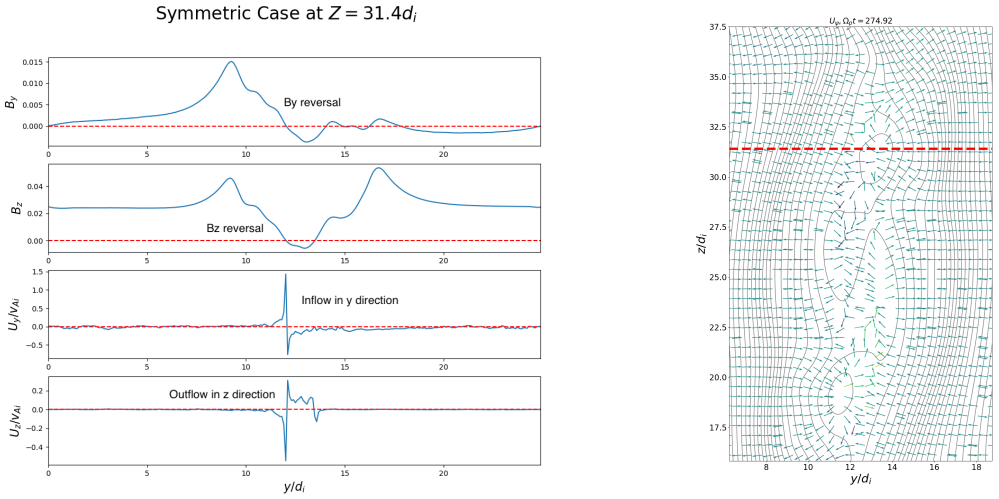

(a) (b)

Figure 3: (a) Line cuts of in-plane magnetic fields and MFT components at the X-line show the magnetic field reversals and the inflow and outflow fluxes. The MFTs are normalized to ion Alfven speed. (b) Dashed red line marks the cut at $Z = 31.4d_i$.

In order to see the magnetic flux and magnetic field reversals, figure 3 show the cuts through the first X-line in Figure 2 at $z = 31.4d_i$ for the symmetric case. The panels are the in-plane magnetic field components (B_y and B_z) and the MFT components (U_y and U_z) normalized by the local ion Alfven speed. The reversals in B happens around $y = 12d_i$ which is accompanied by reversals in magnetic flux with inflow mostly in Y direction and outflow seen mostly in Z direction. The MFT terms (inflow and outflow) are in the order of local ion Alfven speed.

In each step of the simulation output as KHI evolves, we count the number of X-lines manually (in one vortex structure since they are similar due to periodic boundary conditions in z) based on the MFT method (converging inflow and diverging outflow), topology of the magnetic field lines and finding the minimum in-plane magnetic field values below 10^{-4} threshold. We should observe all three criteria in order to count the site as an X-line. We have total of 34 outputs for each simulation with approximately $10\Omega_p$ frequency between the outputs. Figure 4 shows the number of X-lines as a function of time for both simulation cases. The blue line represents the symmetric case and the orange line shows the asymmetric case. At both cases, the reconnection signatures starts appearing around the same time which is when KHI vortices are becoming nonlinear and getting rolled up. Then the reconnection signatures increase and peak during the turbulent phase. Later on, the number of reconnection signatures start to decrease and finally disappear at very late stages of turbulence when vortices are broken into smaller structures. Figure 5 shows the stages of KHI when reconnection signature start, peak and disappear. This analysis shows that the reconnection signatures disappear earlier in the asymmetric density case. It also shows that as the KHI becomes very turbulent and vortices break into smaller structures, the reconnection sites and X-lines become less prevalent until they disappear. We should note that these cases are resembling the northward IMF in Earth's magnetopause boundary and the situation could be different for a southward IMF during turbulent phases of a KHI.

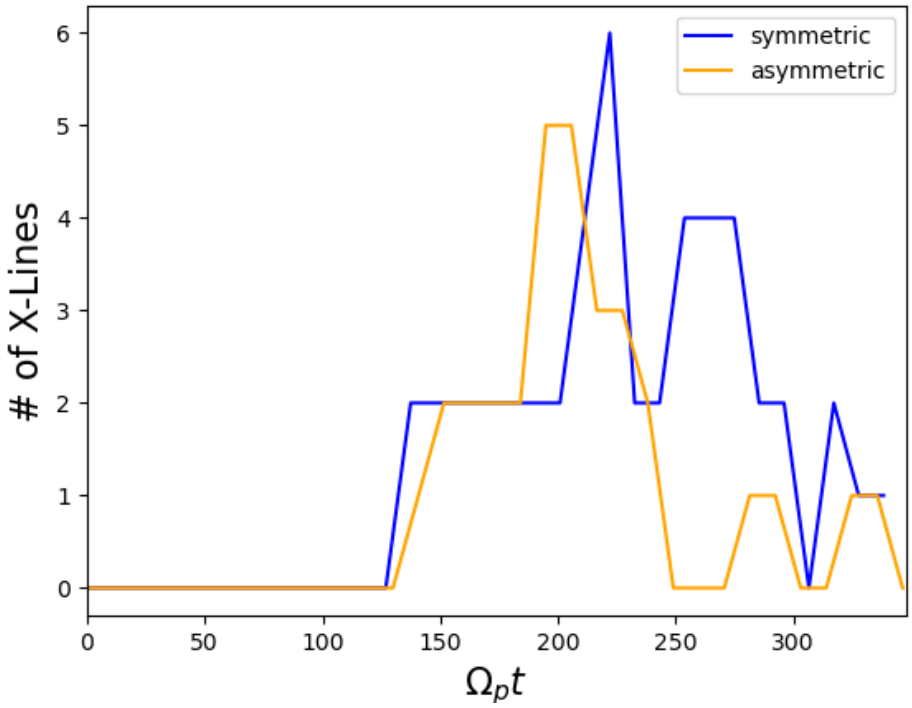

Figure 4: Number of X-lines at one vortex at different stages of KHI evolution. Reconnection signatures starts to appear around the same time in both simulation cases. In asymmetric density case, the reconnection signatures disappear earlier than symmetric case.

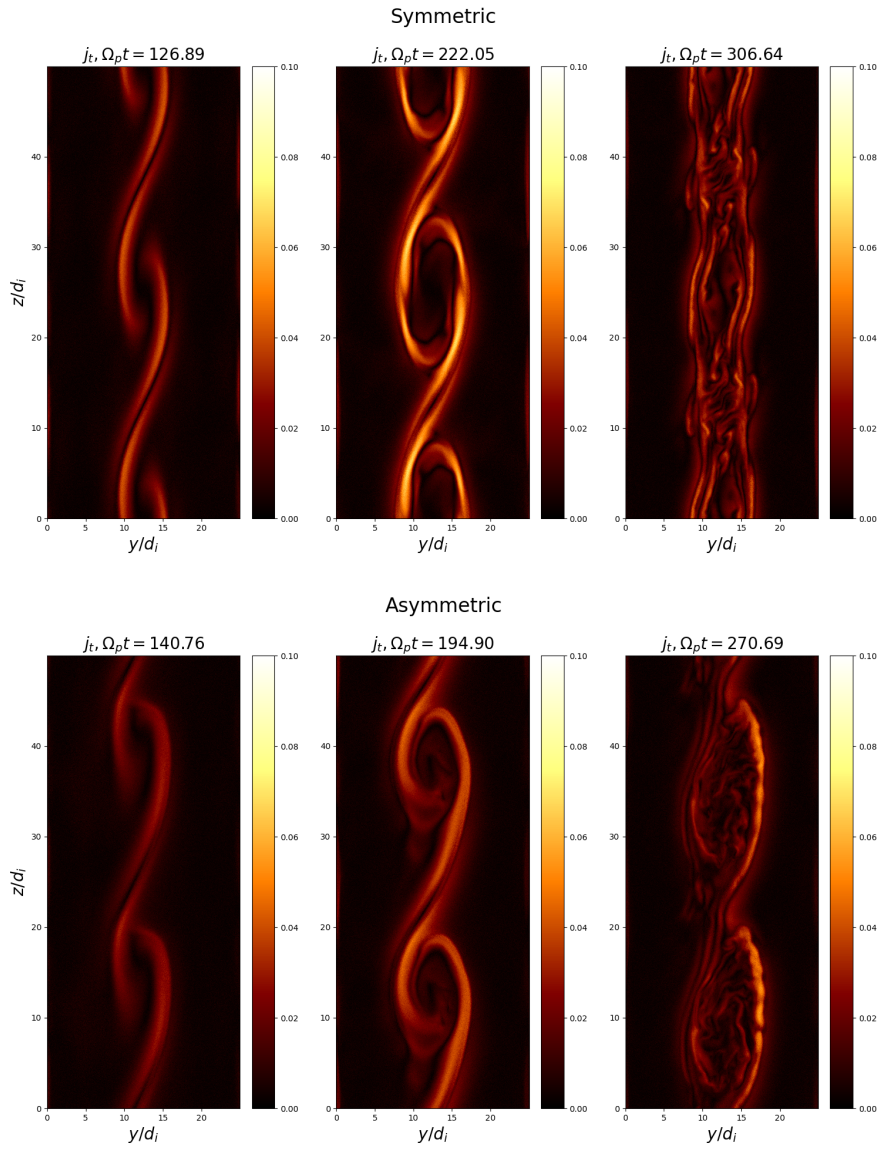

Figure 5: Evolution of total current density in different stages of KHI for symmetric (top) and asymmetric (bottom). First column shows the onset of reconnection signatures. Second column is when the reconnection X-lines peaks and third column is when reconnection signatures disappear.

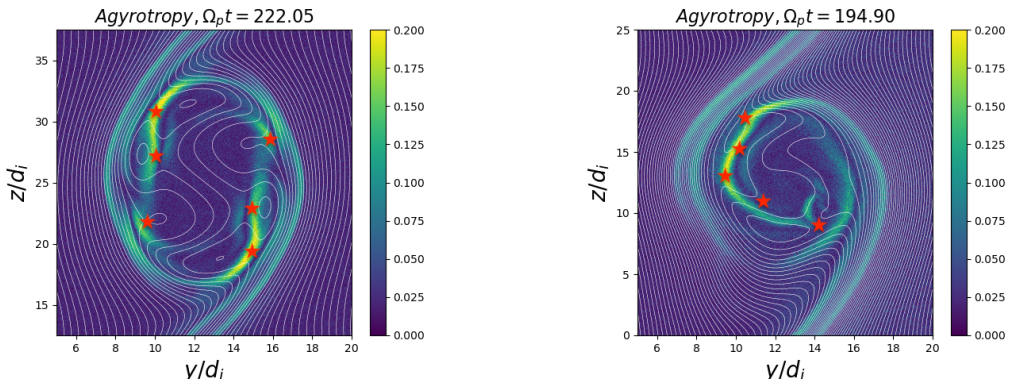

(a) Symmetric (b) Asymmetric

Figure 6: Agyrotropy measurement for symmetric (left) and asymmetric (right) cases. The agyrotropy lights up at the edges of the vortex roll up where the X-lines are seen in both cases. The red stars mark the location of the X-lines.

We also investigate the type of reconnection signatures observed in our PIC simulations. Based on Nakamura et al. (2013), reconnection signatures were observed at the spine regions of the vortices where compressed current sheets where formed in converging flows (type-I) and Nykyri and Otto (2001) showed that reconnection could also happen within the vortex structures when they roll up (type-II). To locate where reconnection is happening, we use the agyrotropy measures (Swisdak, 2016). Agyrotropy in an arbitrary Cartesian system is given by $Q = 1 - 4I_2/((I_1 - P_{||})(I_1 + 3P_{||}))$ where $I_1 = P_{xx} + P_{yy} + P_{zz}$ is trace of pressure tensor and $I_2 = P_{xx}P_{yy} + P_{xx}P_{zz} + P_{yy}P_{zz} - (P_{xy}P_{yx} + P_{yz}P_{zy} + P_{xz}P_{zx})$ sum of principal minors. Agyrotropy shows the asymmetry of the electron pressure tensor in the plane perpendicular to magnetic field due to reconnection. The agyrotropy is known to be enhanced within the reconnection layer such as near the X-lines and separatrices (Swisdak, 2016). Figure 6 displayes the agyrotropy measured in the simulation for both symmetric (left) and asymmetric (right) cases of KHI. In both cases, the agyrotropy lights up and is the strongest at the edges of the vortex roll up where the opposing field lines are. This result is in agreement with Nykyri and Otto (2001) observations of reconnection in the KHI which is type-II reconnection.

Wilder et al. (2023) performed a similar analysis using MMS observations. They showed that reconnection signatures decreases for events further down the magnetospheric flanks and they concluded that as the instability develops into turbulence, reconnection becomes less prevalent. We should point out that Wilder et al. (2023) investigated the reconnection type-I happening in the spine regions of the KHI using MMS observations while the reconnection signatures observed in our simulations happen at the edges of and within the vortex which are type-II reconnection. Our simulations suggest that the reconnection of type-II will also subside with the KHI development and it is in general agreement with Wilder et al. (2023). Therefore according to simulations and MMS observations of the KHI, we suggest that both Type-I and Type-II reconnections should be less likely over time as KHI evolves.

4 Summary and Conclusions

This work studies the presence of reconnection signatures and X-lines in the KHI evolution using 2D PIC simulations. Two cases of PIC simulations with different initial

conditions in density and temperature were investigated. The first simulation case started with homogeneous density and temperature profile in the simulation box called symmetric case. The second simulation had a nonuniform density and temperature profiles resembling a magnetosheath to magnetosphere crossing where KHIs are observed in Earth's magnetosphere. Both simulation cases had a large component of magnetic field pointing out of the plane resembling a northward IMF. Therefore, the reconnections happening in the KHI are high guide field reconnection. All other initial conditions are similar for both cases. With these setups, we can investigate the impact of the symmetry and asymmetry on the reconnection signatures in the KHI evolution and also compare the simulation results with the reported MMS observations (Wilder et al., 2023).

We used the MFT method, the in-plane magnetic field line topology and the in-plane magnetic field magnitude minimums below 10^{-4} threshold to locate the reconnection sites and X-lines. The MFT measures the magnetic flux transported into and out of the reconnection site around the X-lines. We observed the inflow and outflow regions of the flux using the components of MFT indicating where the reconnection is happening and where the X-lines were located. The in-plane magnetic field lines and magnetic field minimums also confirmed the presence of an X-line. Employing these methods, we measured the number of X-lines during the KHI development. Our results indicates that the reconnection signatures start to appear when KHI is nonlinear. This is when the vortices are rolling up. The X-line count and reconnection signatures peak when vortices are completely rolled up and the plasma is getting turbulent. When vortices are broken into smaller structures and the plasma is fully turbulent, the reconnection signatures start to fade away. This is observed in both simulation cases. Both cases have similar onset times for reconnection signatures. But our simulation suggests that the reconnection signatures disappear earlier in the asymmetric case. The asymmetry could help with the KHI getting to the turbulent phase faster. Our results show that the reconnection signatures decrease at the very late stages of the KHI.

We also studied where the reconnection was happening in the KHI structures. We used agyrotropy to find the location of the X-lines in the reconnection site. Agyrotropy enhances in the X-line and separatrix regions when reconnection is happening. We observe that agyrotropy lights up in the compressed current sheets at the edges of the vortex roll ups and within the vortices. Our simulations is in agreement with Nykyri and Otto (2001) and we observe type-II reconnection signatures in our simulations.

Our simulation results are in qualitative agreement with Wilder et al. (2023) using MMS observations. Wilder et al. (2023) showed that the reconnection of type-I (at the spine regions) decreases for KHI events further down the flank when the KHI were more evolved and turbulent. The reconnection signatures observed in our simulations happen at the edges of and within the vortex, of the type reported by Nykyri and Otto (2001) when we start the simulation with a parallel in-plane magnetic field across the flow shear. We suggest that reconnection signatures of type-II will also fade away with time and it is in general agreement with Wilder et al. (2023). Simulations and MMS observations of the KHI suggest that both Type-I and Type-II reconnections should be less likely over time as KHI evolves.

Future work will investigate the impact of IMF strength and in-plane magnetic field geometry on the reconnection signatures in the KHI.

5 Open Research

The data that support the findings of this study are available in NASA HECC. The simulation data are available in this zenodo repository https://doi.org/10.5281/zenodo.10854574.

Acknowledgments

This work was supported by the NASA MMS project and NASA Grant 80NSSC18K1359. Computations were performed on Pleiades at the NASA Advanced Supercomputing.

References

Axford, W., & Hines, C. (1961). A unifying theory of high-latitude geophysical phenomena and geomagnetic storms. *Can. J. Phys.*, *39*(10). doi: https://doi.org/10.1139/p61-17

Eriksson, S., Lavraud, B., Wilder, F. D., & et al. (2016). Magnetospheric multiscale observations of magnetic reconnection associated with kelvin-helmholtz waves. *Geophys. Res. Lett.*, *43*, 5606–5615.

Eriksson, S., Ma, X., Burch, J. L., Otto, A., Elkington, S., & Delemere, P. (2021). Mms observations of double mid-latitude reconnection ion beams in the early non-linear phase of the kelvin-helmholtz instability,. *Front. Astron. Space Sci.*, *8*. doi: 10.3389/fspas.2021.760885

Germaschewski, K., Fox, W., Abbott, S., Ahmadi, N., & et al. (2016). The plasma simulation code: A modern particle-in-cell code with patch-based load-balancing. *J. Comp. Phys.*, *318*.

Hasegawa, H., Fujimoto, M., Phan, T., & et al. (2004). Transport of solar wind into earth's magnetosphere through rolled-up kelvin-helmholtz vortices. *Nature*, *430*(755). doi: 10.1038/nature02799

Hasegawa, H., Fujimoto, M., Takagi, K., & et al. (2006). Single-spacecraft detection of rolled-up kelvin-helmholtz vortices at the flank magnetopause. *J. Geophys. Res.*, *111*. doi: 10.1029/2006JA011631

Hasegawa, H., Retino, A., Vaivads, A., & et al. (2009). Kelvin-helmholtz waves at the earth's magnetopause: Multiscale development and associated reconnection. *J. Geophys. Res.*, *114*. doi: 10.1029/2009JA014042

Johnson, J. R., Wing, S., & Delamere, P. A. (2014). Kelvin helmholtz instability in planetary magnetospheres. *Space Sci. Rev.*, *184*, 1-31. doi: 10.1007/s11214-0140085-z

Karimabadi, H., Roytershteyn, V., Wan, M., Matthaeus, W. H., Daughton, W., Wu, P., & et al. (2013). Activity of superior colliculus in behaving monkey. ii. effect of attention on neuronal responses. *Phys. Plasmas*, *20*(12303). doi: 10.1063/1.4773205

Kavosi, S., & Raeder, J. (2015). Ubiquity of kelvin-helmholtz waves at earth's magnetopause. *Nat. Commun.*, *6*(7019). doi: 10.1038/ncomms8019

Li, T. C., Liu, Y., & Qi, Y. (2021). Identification of active magnetic reconnection using magnetic flux transport in plasma turbulence. *The Astrophysical Journal Letters*, *909*. doi: 10.3847/2041-8213/abea0b

Liu, Y.-H., & Hesse, M. (2016). Suppression of collisionless magnetic reconnection in asymmetric current sheets. *Physics of Plasmas*, *23*. doi: 10.1063/1.4954818

Liu, Y.-H., Hesse, M., Guo, F., Li, H., & Nakamura, T. K. M. (2018). Strongly localized magnetic reconnection by the super-alfvénic shear flow. *Physics of Plasmas*, *25*. doi: 10.1063/1.5042539

Ma, X., Delamere, P., Otto, A., & Burkholder, B. (2017). Plasma transport driven by the three dimensional kelvin-helmholtz instability. *J. Geophys. Res.*, *122*, 10382–10395. doi: https://doi.org/10.1002/2017JA024394

Nakamura, T. K. M., & Daughton, W. (2014). Turbulent plasma transport across the earth's low-latitude boundary layer. *Geophysical Research Letters*, *41*(24), 8704.

Nakamura, T. K. M., Daughton, W., Karimabadi, H., & Eriksson, S. (2013). Three-dimensional dynamics of vortex-induced reconnection and comparison with themis observations. *Geophys. Res. Space Physics*, *118*, 5742–5757. doi: 10.1002/jgra.50547

Nykyri, K., & Otto, A. (2001). Plasma transport at the magnetospheric boundary due to reconnection in kelvin-helmholtz vortices. *Geophys. Res. Lett.*, *28*, 3565–3568. doi: 10.1029/2001GL013239

Nykyri, K., Otto, A., Lavraud, B., Mouikis, C., Kistler, L. M., Balogh, A., & Rème, H. (2006). Cluster observations of reconnection due to the kelvin-helmholtz instability at the dawnside magnetospheric flank. *Ann. Geophys.*, *24*, 2619. doi: 10.1029/2001GL013239

Pritchett, P. L., & Coroniti, F. V. (1984). The collisionless macroscopic kelvin-helmholtz instability 1.transverse electrostatic mode. *J. Geophys. Res.*, *89*, 168–178.

Qi, Y., Li, T. C., Russell, C. T., & et al. (2022). Magnetic flux transport identification of active reconnection: Mms observations in earth's magnetosphere. *The Astrophysical Journal Letters*, *926*. doi: 10.3847/2041-8213/ac5181

Stawarz, J. E., Eriksson, S., Wilder, F. D., Ergun, R. E., Schwartz, S. J., Pouquet, A., & et al. (2016). Observations of turbulence in a kelvin-helmholtz event on 8 september 2015 by the magnetospheric multiscale mission. *J. Geophys. Res. Space Phys.*, *121*. doi: 10.1002/2016JA023458

Swisdak, M. (2016). Quantifying gyrotropy in magnetic reconnection. *Geophys. Res. Lett.*, *43*, 43–49. doi: 10.1002/2015GL066980

Wilder, F. W., King, A., Gove, D., & et al. (2023). The occurrence and prevalence of magnetic reconnection in the kelvin-helmholtz instability under various solar wind conditions. *Journal of Geophysical Research: Space Physics*, *128*(10). doi: https://doi.org/10.1029/2023JA031583